

## RECOMBINATION IMAGING OF III-V SOLAR CELLS

G.F. Virshup  
Varian Research Center  
Palo Alto, California

An imaging technique based on the radiative recombination of minority carriers in forward-biased solar cells has been developed for characterization of III-V solar cells. The initial use of this technique has been to determine the quality of 1.93-eV AlGaAs solar cells grown by metalorganic chemical vapor deposition (MOCVD). The solar cells are forward biased until the  $J_{sc}$  reaches a threshold of approximately 100 mA/cm<sup>2</sup>. At this current, the light emitted by 1.93-eV AlGaAs cells due to radiative recombination is sufficiently bright to be seen visually. Variations in the intensity of the light across the wafer and individual cells correlates well with various loss mechanisms. The technique is especially suited to high-bandgap cells because the emitted radiation is visible in the spectrum and the image can be recorded using regular photographic film. GaAs cells have been studied with this technique using vidicon tubes with responsivity as low as 1.15 eV.

## INTRODUCTION

III-V solar cells are being developed at Varian for use in multijunction solar cells. The successful development of these cells requires an understanding of the loss mechanisms which detract from the optimal performance of the cells. Imaging the photons generated by recombination of injected minority carriers during forward biasing of solar cells has led to the identification of various loss mechanisms. Recombination images are spatial views of cell current and loss mechanisms which simplify the interpretation of complementary electrical data such as open circuit voltage, short circuit current, efficiency, and fill factor. Data which lead to the identification of three loss mechanisms in 1.93-eV AlGaAs cells grown by metalorganic chemical vapor deposition (MOCVD) is presented.

## EXPERIMENTAL DESCRIPTION

Recombination imaging (RI) is based on the radiative recombination of minority carriers in forward-biased solar cells. This process occurs in direct-gap solar cells such as those in the GaAs material system. When these cells are forward biased, there is injection of minority carriers across the p-n junction. As seen in Ref. 1, these carriers recombine by both radiative and nonradiative processes, relative occurrences of which are dependent on the two associated lifetimes.

The radiative recombination process yields photons having bandgap energy of the semiconducting material. A fraction of these photons escape the semiconductor. For high-bandgap materials such as 1.93-eV AlGaAs, the emitted photons can be detected by the human eye; however, an infrared viewing scope is required for viewing images from lower energy bandgap materials. For permanent images, photographic paper can record visible photons and vidicon camera image photons with energies as low as 1.15 eV.

The spatial variations of the recombination image intensity indicate regions of high or low radiative recombination, which allows qualitative evaluation of the cell quality. A schematic for setting up a RI system is shown in Fig. 1. The power supply forward biases the cell under test to a predetermined current or voltage level, at which time the imaging system produces a recombination image.

#### CHARACTERIZATION OF III-V SOLAR CELLS

Initial use of recombination imaging at Varian has been in the characterization of AlGaAs solar cells with bandgaps of 1.93 eV. The cells are grown by MOCVD on Bridgman D-shaped GaAs wafers. Under forward biasing, these cells emit 642-nm photons which are visible as red light.

Figures 2 and 3 are composites of recombination images of the solar cells processed from two different MOCVD growths. The cells in these figures were imaged using forward bias currents of 100 and 400 mA/cm<sup>2</sup>, respectively. The composites allow us to see growth nonuniformities over the entire wafer. Gas flows were from right to left during the growth of both wafers.

The left side in Fig. 2 shows reduced intensity of light emission. This is interpreted as a downstream depletion of trimethylgallium and consequently higher aluminum fraction in the AlGaAs layers during growth, which results in a transition from direct to indirect AlGaAs. The recombination image of indirect gap material is of extremely low intensity due to the radiative lifetime in indirect material, as seen in Ref. 2. AlGaAs makes the transition from direct-gap material to indirect-gap material near 1.94 eV. These results are supported by photoluminescence measurements of these samples.

Table I contains the efficiency, open circuit voltage ( $V_{oc}$ ), short circuit current ( $J_{sc}$ ), and fill factor (FF); the information corresponds to the cells in Fig. 2. The efficiencies of the cells ranges from 2% to over 10%, with 50% of the cells between 9 and 10.5% efficiency. The average current density of these cells over the wafer is 12 mA/cm<sup>2</sup>, while the average  $V_{oc}$  is 1.37 volts. The poor cells (efficiencies < 9%) all exhibit lower fill factors, but some (2, 6, 7, 11) have low values of  $I_{sc}$  and others (cells #9, 10) have low  $V_{oc}$ . The terminal electrical characteristics identified a problem with some of the cells, but did not explain the cause of the loss mechanisms. The causes only became clear when recombination images were compared to the electrical characteristics.

The cells with reduced image intensity (cells #2, 6, 7, 11) have an average current density of only 8 mA/cm<sup>2</sup>. The lower current density correlates well with either a higher bandgap semiconductor or a lower quantum yield, both of which are expected for the indirect-bandgap material.

Another loss mechanism seen in Fig. 1 is the existence of point defects. These are visualized as localized dark regions scattered over the wafer. Some point defects were found to be shorting paths which lowered the open circuit voltage of the cells. Other point defects are just surface defects which block light from exiting or entering the cells. Cells 9 and 10 exhibit low open circuit voltages due to the shorting defects, while their current density is not affected. The point defects seen in cells 8 and 14 are surface defects. Also seen in Fig. 1 are disconnected grid lines which are visualized as dark regions due to the lack of current flow in the nearby regions.

Similar loss mechanisms have been seen with recombination imaging in other 1.93-eV AlGaAs growths. Figure 3 shows a wafer with downstream direct-to-indirect transition, but few point defects.

Recombination imaging has been implemented for GaAs cells whose bandgap radiation of 870 nm is beyond the sensitivity of regular photographic paper. Figure 4 is a recombination image of a GaAs space cell made using a vidicon camera with sensitivity to wavelengths as long as 1100 nm. Figure 4 also shows that point defects and disconnected grid lines can be detected in GaAs solar cells.

#### SUMMARY

Recombination imaging of solar cells is a simple technique that allows visual identification of direct-gap solar cell loss mechanisms. When used in mapping of whole wafers, it has helped identify three independent loss mechanisms (broken grid lines, shorting defects, and direct-to-indirect bandgap transitions), all of which resulted in lowered efficiencies. The imaging has also lead to improvements in processing techniques to reduce the occurrence of broken gridlines as well as surface defects. The ability to visualize current mechanisms in solar cells is an intuitive tool which is powerful in its simplicity.

#### REFERENCES

1. Sze, S. M.: Physics of Semiconductor Devices, Second Edition, John Wiley and Sons, New York, 1981.
2. Muller, R. S.; and Kamins, T. I.: Device Electronics for Integrated Circuits, John Wiley and Sons, New York.

TABLE I: Map of current-voltage measurement results from wafer shown in Fig. 2.

cell #	2	3		5	
Effic (%)	5.02	9.17		9.03	
Voc (V)	1.34	1.39		1.37	
Jsc(mA/cm)	8.1	11.6		12.0	
FF	0.62	0.77		0.74	
6	7		8	9	10
4.91	6.57		10.3	2.14	4.80
1.34	1.37		1.38	0.43	1.28
6.3	8.94		12.3	12.3	11.7
0.78	0.72		0.82	.51	0.43
11	12		14	15	
6.09	9.72		10.3	10.5	
1.35	1.38		1.36	13.7	
7.79	11.30		13.8	12.5	
0.78	0.84		0.80	0.83	

← ← GAS FLOW ← ←

ORIGINAL PAGE IS  
OF POOR QUALITY.

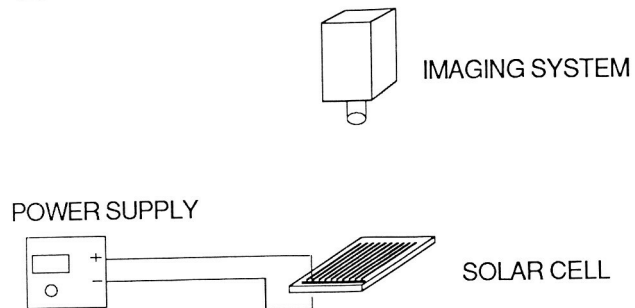


Fig. 1 Schematic of recombination imaging system.

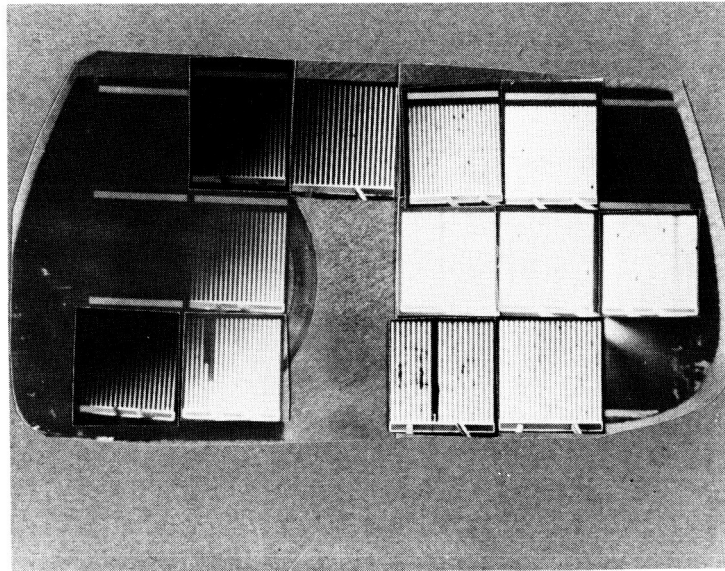


Fig. 2 Recombination image of 1.93-eV AlGaAs solar cells with  $100 \text{ mA/cm}^2$  forward current.

ORIGINAL PAGE IS  
OF POOR QUALITY

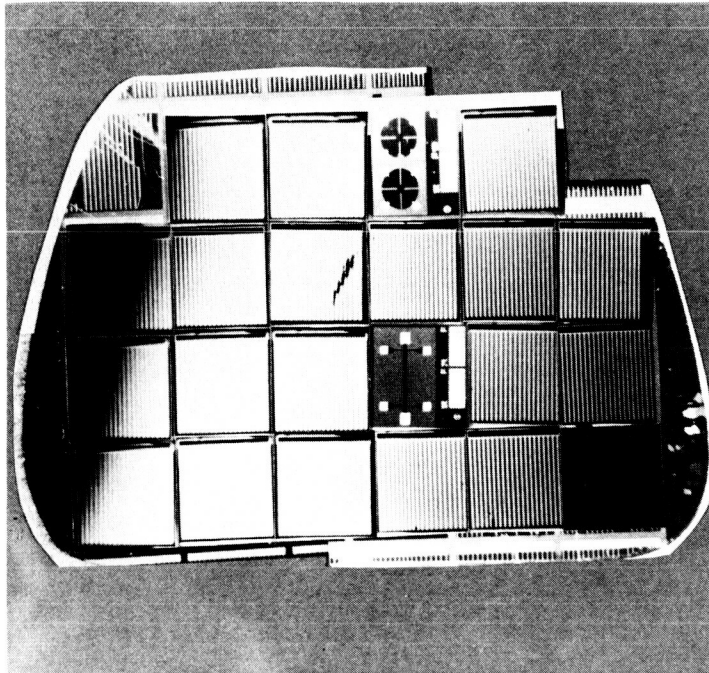


Fig. 3 Recombination image of 1.93-eV AlGaAs solar cells  
with  $400 \text{ mA/cm}^2$  forward current.

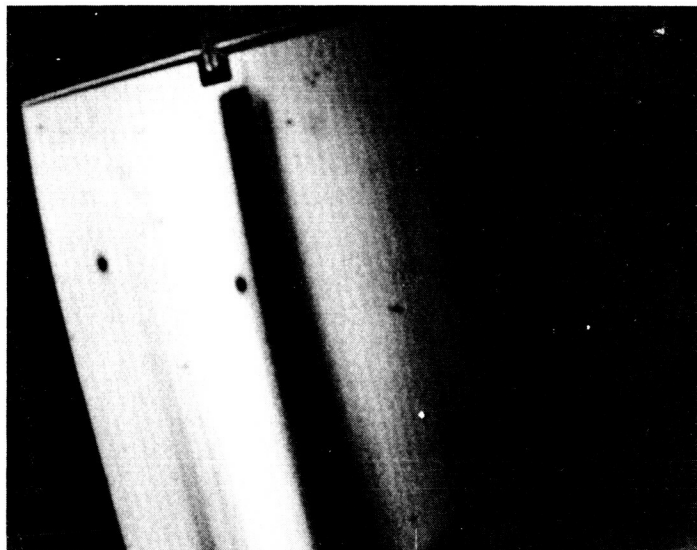


Fig. 4 Recombination image of GaAs space cell.  
Imaged using vidicon tube.